WYOMING STATE GEOLOGICAL SURVEY
Wallace L. Ulrich, Director and Sate Geologist
Laramie, Wyoming

Geology - Interpreting the past - providing for the future

Prepared in cooperation with the U.S. GEOLOGICAL SURVEY

Open File Report 11-7
Best Ranch 1:24,000 - scale Bedrock Geologic Map

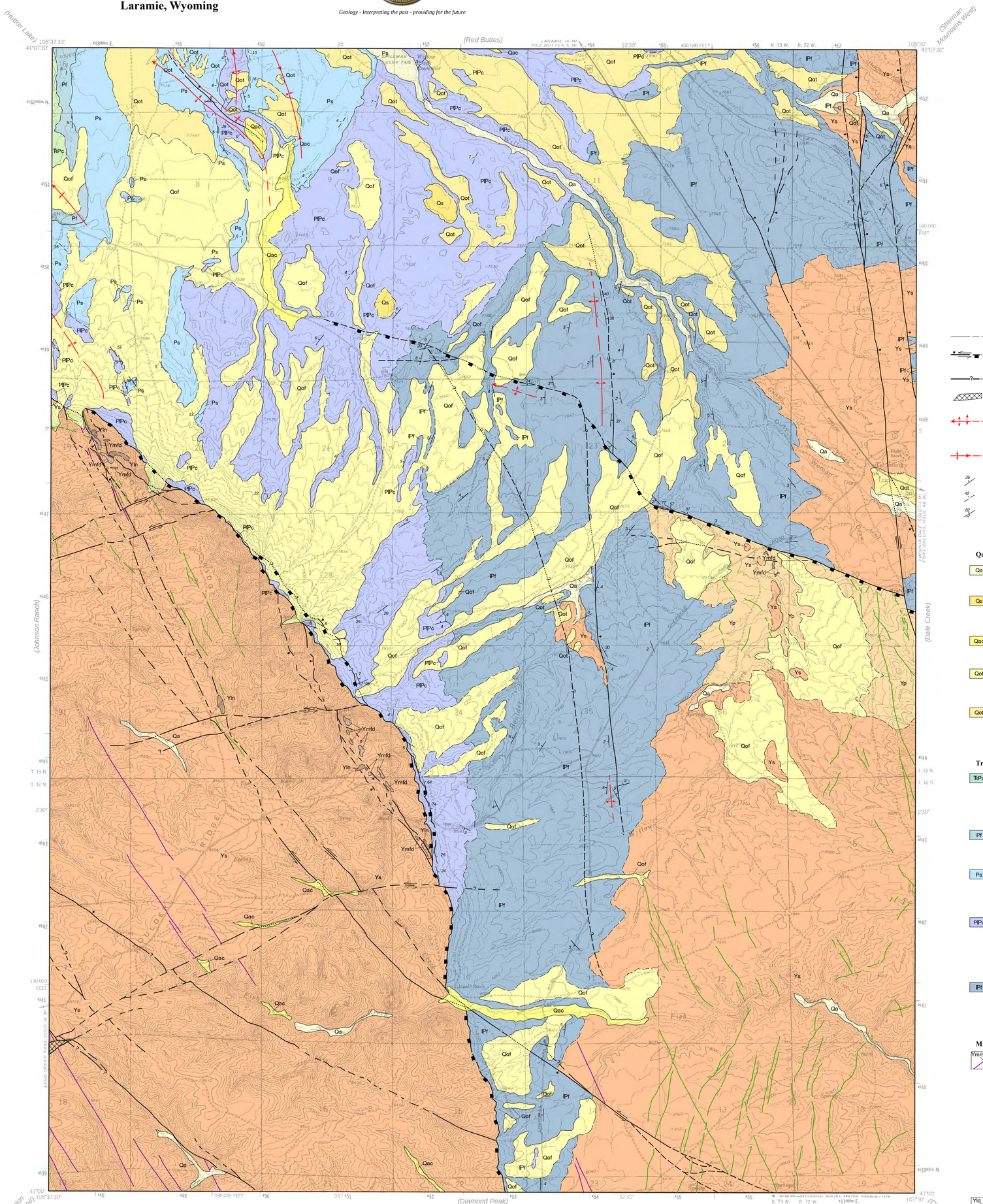

PRELIMINARY GEOLOGIC MAP OF THE BEST RANCH QUADRANGLE, ALBANY COUNTY, WYOMING

by
Alan J. Ver Ploeg, Davin Bagdonas, and J. Fred McLaughlin
2011

EXPLANATION

CORRELATION OF MAP UNITS

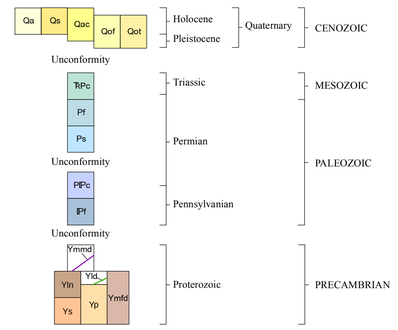

MAP SYMBOLS

Formation contact—Dashed where approximately located

Fault—Dashed where approximately located, dotted where concealed; block on the hanging wall of reverse fault; bar and ball on downthrown block; arrows indicate relative direction of oblique-slip movement

Fracture or possible fault—Dashed where approximately located, dotted where concealed

Fault Zone—Characterized by brittle deformation; fault breccia, cataclastic material, and alteration is common

Anticline—Dashed where approximately located; arrow on end indicates direction of plunge; on asymmetrical structure shorter arrow indicates steeper dipping limb trace of axial plane as determined by field measurements and aerial photo interpretation

Syncline—Dashed where approximately located, dotted where concealed; arrow on end or along axis indicates direction of plunge

Strike and dip of inclined bedding—With angle of dip

Strike and dip measurements from Nicoll, 1963—With angle of dip

Strike and dip of overturned bedding—With angle of dip

DESCRIPTION OF MAP UNITS

Quaternary surficial deposits

Qa **Alluvial deposits (Holocene)**—Unconsolidated to poorly consolidated clay, silt, sand, and gravel, mainly in flood plains and lower stream terraces. Alluvial material is derived from all local geologic units. Thickness approximately 0 to 50 feet (15 m) (Nicoll, 1963)

Qs **Windblown sand deposits (Holocene)**—Active and stabilized dunes, made up of very fine- to fine-grained sand sourced by Casper Formation sandstones. Buff to gray to reddish, locally covered with patchy vegetation. Dunes are primarily deposited around vegetation, bedrock outcrops, and in small washes. Thickness 0 to 10 feet (3 m) (Nicoll, 1963)

Qac **Mixed alluvium and colluvium (Holocene/Pleistocene)**—Sand, silt, clay, and gravel deposited along intermittent streams; includes slope wash and smaller alluvial fan deposits that coalesce with alluvium. Thickness 0 to 50 feet (15 m) (Nicoll, 1963)

Qof **Older alluvial fan deposits (Pleistocene)**—Poorly sorted clay, silt, sand, and gravel; crudely bedded to non-bedded with some component of debris flow. Includes boulders and cobbles of local geologic units. Currently inactive and dissected, often occurring as erosional remnants. Thickness 0 to 10 feet (3 m) (Nicoll, 1963)

Qot **Older terrace deposits (Pleistocene)**—Beds of course sand and gravel with occasional boulders and lenses of silt and clay. Resistant limestone and granite material occur as rounded, well-weathered boulders and gravels. Often occur as erosional remnants ranging from 20 to 300 feet (6 to 91 m) above present stream flood plains. Some remnants may actually be older alluvial fan remnants. Thickness 0 to 10 feet (3 m) (Nicoll, 1963)

Triassic, Permian, and Pennsylvanian sedimentary rocks

TrPc **Chugwater Formation (Triassic and Permian)**—Red shale and siltstone with interbedded red to salmon to buff, fine-grained sandstone in upper part. Lower part of section contains red shale and calcareous siltstone, interbedded with thin to thick gypsum beds, local solution breccia, and banded wavy gypsiferous limestone sometimes mistaken as part of the Forelle Limestone. This part of the Chugwater Formation, along with the underlying Forelle Limestone and Satanka Shale, is mapped as Goose Egg Formation west of the Laramie Basin. Thickness 660 to 1000 feet (201 to 305 m) (Nicoll, 1963)

Pf **Forelle Limestone (Permian)**— Gray to purple, thin-bedded, sparsely fossiliferous, resistant limestone locally interbedded with red siltstone and thin gypsum beds. Wavy outcrops of algal dome structure and more crinkly contorted bedding common (Nicoll, 1963). Outcrops as low, broken, small ridges and highly fractured beds. Thickness 4 to 20 feet (1 to 6 m) (Nicoll, 1963)

Ps **Satanka Formation (Permian)**— Red siltstone and shale that is often banded with white and ocher colored zones, and buff to orange to red fine-grained soft sandstone with distinct ripple marks common near the base of the unit. Unconformably overlies the Casper Formation. Contact with Casper Formation can be difficult to discern though changes in grain angularity and ripple size are common along the contact boundary. Thickness 75 to 260 feet (23 to 79 m) (Nicoll, 1963; Ver Plog, 1999a)

PPc **Casper Formation (Permian and Pennsylvanian)**—Buff to reddish, calcareous to quartzitic, very fine- to course-grained, well-cemented sandstone interbedded with thin buff to purplish-gray limestone and dolomite beds, usually micritic and locally fossiliferous. Sandstone often exhibits large-scale festoon cross-bedding with siliceous fracture fill associated with faulting and local stresses. Within the map area Casper Formation outcrops as distinct resistant ridges, anchoring abundant vegetation and thick brush. Thickness is highly variable within the Laramie Basin, thinning toward the southwest. Within the map area thickness is 100 to 250 feet (30 to 79 m) (Nicoll, 1963)

IPf **Fountain Formation (Pennsylvanian)**—Course-grained pink to red to purple sandstone and arkose, with some conglomerates, fossiliferous limey-sandstones, siltstones, shales, and thin limestone lenscs. Blotchy pink-red iron staining is common on arkosic, resistant, ridge forming portions of the formation. Interfingers with and underlies Casper Formation. Thickness is variable within the Laramie Basin, thickening toward the southwest. Within the map area thickness is 10 to 400 feet (3 to 122 m) (Nicoll, 1963)

Middle Proterozoic granitic and metamorphic rocks

Ymmd **Monzodiorite dike (Mg-rich)**—Fine-grained, brown to purple-black, highly fractured and weathered monzodiorite dikes that outcrop linearly for hundreds of meters to several kilometers through the Sherman batholith. Dikes are predominately sub-vertically oriented, which can be easily seen in the field as vertical to near vertical jointing within the dike. Monzodiorite dikes contain megacrystic alkali feldspars that display thin rims of plagioclase. Plagioclase xenocrysts associated with small, round quartz grains and hornblende are seen in random locations in the field (Frost, and others, 1999). Two varieties of monzodiorite dikes have been recognized within the Sherman batholith that include an Fe-rich commingled body and an Mg-rich body that has less interaction with local country rock (Edwards, 1993). Mg-rich dikes are common within the area of the quadrangle. Monzodiorite dikes in the quadrangle contain xenocrysts as described above, in addition to plagioclase and perthite that show obvious compositional zoning. Abundant, very small, needle-shaped apatite are pervasive throughout the sample and can be seen in thin section.
Major Phases include plagioclase (some as myrmekite), perthite, microcline, biotite (sometimes altered to chlorite), hornblende, quartz, and orthoclase.
Minor Phases include apatite, epidote, ilmenite, magnetite, and titanite.
The monzodiorite dikes have not been dated using modern isotope concordia methods. However, monzodiorite dikes cross-cut Sherman Granite, Lincoln Granite enclaves and dikes, and porphyritic granite indicating a post-Sherman batholith emplacement history.

Yld **Leucocratic dike**—Fine- to large-grained, sub-round to angular crystal structures of quartz, plagioclase and microcline with small amounts of mafic minerals. Some outcrops show localized mafic mineral concentrations along grain boundaries of primary quartz and plagioclase crystals. Leucocratic dikes range from fine- to small-grained, pink-red, granitic, late-stage batholith injections to large-grained, maturely inner-grown crystal structures that consist of large quartz and alkali feldspar grains. Hydrothermal fluid alteration is evident in the larger crystal structure dikes as hematite-staining and epidote. Alteration can also be seen as secondary, subgrain quartz growth within the larger crystal structure and especially along fractures within crystal faces.
Major Phases are plagioclase, quartz, microcline, perthite, and biotite.
Minor Phases are apatite, zircon, hornblende, ilmenite, and fluorite (Frost, and others, 1999).
The age of the leucocratic dikes is similar to that of the Lincoln Granite and in many cases the two are compositionally similar. The age of the fine-grained leucocratic dikes is assumed to be similar to the Lincoln Granite at 1,430 + 2.6 Ma (Mega-annum or million years before present) by U-Pb dating (Frost, and others, 1999). The age of the larger-grained leucocratic dikes is unknown, but field relationships suggest late-stage batholith emplacement as a partially differentiated end member of the Sherman batholith.

Yln **Lincoln Granite**—Medium- to small-grained, equigranular, orange-red to orange-gray, biotite granite that outcrops in horizontal sheets with resistant caps that create hills, domes, and high ridges that tend to outcrop above Sherman Granite. Some Lincoln Granite occurs as dikes and small inclusions/enclaves in the adjacent Sherman Granite. Lincoln Granite is generally less abundant than Sherman Granite. Lincoln Granite is a more evolved phase of the Sherman batholith with greater silica and less iron enrichment. The Lincoln Granite is classified as a ferroan alkali-calcic peraluminous granitoid (Frost, and others, 2001). Contacts with the Sherman Granite are generally sharp. Contacts with the porphyritic granite are mingled to sharp. The Lincoln Granite was named after the Lincoln Monument that is present on the summit of the old Lincoln Highway and Interstate 80 (Edwards, 1993).
Major Phases are quartz, plagioclase, microcline, perthite, biotite, hornblende, and ilmenite.
Minor Phases are apatite, zircon, myrmekite.
Locally along fractures and faults the Lincoln Granite includes very small needle-like apatite along with titanite, epidote, and minor hematite and chlorite as alteration products. Some samples include isolated alkali feldspar megacrysts that make up less than 1 percent of the rock (Frost, and others, 1999).
The Lincoln Granite has been dated at 1,430 + 2.6 Ma by U-Pb dating (Frost, and others, 1999).

Ymfd **Mafic bodies, pods, and dikes (Fe-rich)**—A small number of Fe-rich pods occur in the quadrangle along Willow Creek on the eastern edge of the map area and as dikes along the northwestern tip of Boulder Ridge on the western edge of the map area. They are strongly commingled with local porphyritic granite and Lincoln Granite and are generally emplaced as enclave-like dike features. Some field samples contain small inclusions of Sherman Granite as well as megacrystic plagioclase. In thin section the megacrystic plagioclase appear to be xenocrysts. Field relationships suggest dike/pod emplacement during batholith cooling.
Major Phases include plagioclase, perthite, biotite, quartz, and orthoclase.
Minor Phases are titanite, apatite, ilmenite, magnetite and zircon.
The monzodiorite dikes have not been directly dated using modern isotope methods. Field relationships as described above suggest a similar intrusive age to the Sherman and porphyritic granites in the range of 1,430-1,433 Ma (Edwards, 1993).

Yp **Porphyritic granite**—Medium-grained, orange-gray to brown biotite-hornblende granite with 0.4 to 1.6 in (1 to 4 cm), orange-pink and pink-gray perthitic microcline, and some plagioclase phenocrysts that show rapakivi-texture of plagioclase and quartz rims. Some outcrops of porphyritic granite show orientation of phenocrysts in a single stress direction that relates to local emplacement deformation. The porphyritic granite, named by Edwards (1993) is considered a modal composition end member between the Sherman and Lincoln Granites (Frost, and others, 1999). Sample locations along Willow Creek include hydrothermally altered rapakivi-texture where the perthitic cores have been altered to a very fine-grained, feathery mass of sericite. Epidote and minor chlorite are also seen as alteration products. Biotite exhibits moderate to heavy chloritic alteration with fine-grained, secondary quartz growth that delaminates cleavage plains. Hematite-rich fluid is evident on crystal faces within the rock and is associated with cross-cutting quartz veins.
Major Phases of the porphyritic granite are perthitic microcline, plagioclase, quartz, biotite, hornblende, and in hydrothermally altered samples, epidote and chlorite.
Minor Phases include ilmenite, apatite, zircon, titanite, pigeonite, and in hydrothermally altered samples sericite, hematite and hydrothermally associated secondary quartz.
The porphyritic granite has been dated at 1,430-1,433 Ma by modal composition association between the Lincoln and Sherman Granites respectively (Frost, and others, 1999).

Ys **Sherman Granite**—Medium- to coarse-grained, pink to reddish-orange, biotite-hornblende granite that outcrops in rounded to craggy mounds and more commonly a thick weathered grus. The Sherman Granite has a subporphyritic granular texture, exhibiting megacrystic microcline rimmed in plagioclase resulting in rapakivi-texture in some locations. Sherman Granite is the most common phase of the Sherman batholith. It is the less evolved phase of the Sherman batholith with lower silica and greater iron concentrations. The Sherman Granite is classified as a ferroan alkali-calcic metaluminous granitoid (Frost, and others, 2001). Contacts with both the Lincoln Granite and the porphyritic granite tend to be sharp.
Major Phases are microcline, plagioclase, quartz, hornblende, biotite, and ilmenite.
Minor Phases include zircon and apatite, and in some locations augite, pigeonite, and fayalite.
The Sherman Granite has been dated at 1,433 ± 1.5 Ma by U-Pb dating (Frost, and others, 1999).

SOURCES OF GEOLOGICAL DATA

Blackstone, D.L., Jr., 1996, Structural geology of the Laramie Mountains, southeastern Wyoming and northeastern Colorado: Wyoming State Geological Survey Report of Investigations 51, 28 p.

Braddock, W.A., Cole, J.C., and Eggler, D.H., 1989, Geologic map of the Diamond Peak quadrangle, Larimer County, Colorado and Albany County, Wyoming: U.S. Geological Survey Geologic Quadrangle Map GQ-1614, scale 1:24,000.

Braddock, W.A., Eggler, D.H., and Courtright, T.R., 1989, Geologic map of the Virginia Dale quadrangle, Larimer County, Colorado and Albany County, Wyoming: U.S. Geological Survey Geologic Quadrangle Map GQ-1616, scale 1:24,000.

Edwards, B.R., 1993, A field, geochemical, and isotopic investigation of the igneous rocks in the Pole Mountain area of the Sherman batholith, southern Laramie Mountains, Wyoming, U.S.A.: M.S. thesis, University of Wyoming, Laramie, 164 p., scale 1:24,000.

Edwards, B.R., and Frost, C.D., 2000, An overview of the petrology and geochemistry of the Sherman batholith, southeastern Wyoming: Identifying multiple sources of Mesoproterozoic magmatism: Rocky Mountain Geology, v. 35, no. 1, p. 113-137.

Eggler, D.H., 1967, Structure and petrology of the Virginia Dale ring-dike complex, Colorado-Wyoming Front Range: Ph.D. dissertation, University of Colorado, Boulder, 154 p., scale 1:62,500.

Eggler, D.H., Larson, E.E., and Bradley, W.C., 1969, Granites, grusses, and the Sherman erosion surface, southern Laramie Range, Colorado-Wyoming: American Journal of Science, v. 267, p. 510-522.

Eggler, D.H., and Braddock, W.A., 1989, Geologic map of the Cherokee Park quadrangle, Larimer County, Colorado and Albany County, Wyoming: U.S. Geological Survey Geologic Quadrangle Map GQ-1615, scale 1:24,000.

Frost, C.D., and Frost B.R., 1997, Reduced rapakivi-type granites: The tholeiite connection: Geology, v. 25, no. 7, p. 647-650.

Frost, C.D., Frost, B.R., Chamberlain, K.R., and Edwards B.R., 1999, Petrogenesis of the 1.43 Ga Sherman Batholith, SE Wyoming, USA: A reduced, rapakivi-type anorogenic granite: Journal of Petrology, v. 40, no. 12, p. 1771-1802.

Frost, B.R., Arculus, R.J., Barnes, C.G., Collins, W.J., Ellis, D.J., Frost, C.D., 2001, A geochemical classification of granitic rocks: Journal of Petrology, v. 42, p. 2033-2048.

Hausel, W.D., Glahn, P.R., and Woodzick, T.L., 1981, Geological and geophysical investigations of kimberlite in the Laramie Range of southeastern Wyoming: Wyoming State Geological Survey Preliminary Report 18, 13 p., plates 1 and 2, scale 1:24,000.

Houston, R.H., and others, 1968, A regional study of rocks of Precambrian age in that part of the Medicine Bow Mountains lying in southeastern Wyoming with a chapter on the relationship between Precambrian and Laramide structure: Wyoming State Geological Survey Memoir 1, 165 p., plate 1, scale 1:63,360.

Love, J.D., and Christiansen, A.C., 1985, Geologic Map of Wyoming: U.S. Geological Survey, scale 1:500,000.

Love, J.D., and Weitz, J.L., 1953, Geologic map of Albany County, Wyoming: Wyoming Geological Association 8th Annual Field Conference Guidebook, unnumbered map, scale 1:158,400 (also published as an unnumbered map by the Wyoming State Geological Survey).

Nicoll, G.A., 1963, Geology of the Hutton Lake anticline area, Albany County, Wyoming: M.S. thesis, University of Wyoming, Laramie, 80 p., plate 1, scale 1:35,200.

Vargas, R., 1974, Photogeologic map of the Jelm Mountain quadrangle, Albany County, Wyoming; M.S. thesis, University of Wyoming, Laramie, 68 p., plate 1, scale 1:24,000.

Ver Ploeg, A.J., 1995a, Preliminary geologic map of the Laramie quadrangle, Albany County, Wyoming: Wyoming State Geological Survey Preliminary Geologic Map Series PGM-95-1, scale 1:24,000.

Ver Ploeg, A.J., 1995b, Preliminary geologic map of the Red Buttes quadrangle, Albany County, Wyoming: Wyoming State Geological Survey Preliminary Geologic Map Series PGM-95-2, scale 1:24,000.

Ver Ploeg, A.J., 1998, Geologic map of the Laramie quadrangle, Albany County, Wyoming: Wyoming State Geological Survey Geologic Map Series MS 50, scale 1:24,000.

Ver Ploeg, A.J., 1999a, Reconnaissance/photogeologic map of the Best Ranch quadrangle, Albany County, Wyoming: Wyoming State Geological Survey files (unpublished), scale 1:24,000.

Ver Ploeg, A.J., 1999b, Reconnaissance/photogeologic map of the Hutton Lake quadrangle, Albany County, Wyoming: Wyoming State Geological Survey files (unpublished), scale 1:24,000.

Ver Ploeg, A.J., 1999c, Reconnaissance/photogeologic map of the Pilot Hill quadrangle, Albany County, Wyoming: Wyoming State Geological Survey files (unpublished), scale 1:24,000.

Ver Ploeg, A.J., 1999d, Reconnaissance/photogeologic map of the Sherman Mountains West quadrangle, Albany County, Wyoming: Wyoming State Geological Survey files (unpublished), scale 1:24,000.

Zielinski, R.A., Peterman, Z.E., Stuckless, J.S., Rosholt, J.N., and Nkomo, I.T., 1981, The chemical and isotopic record of rock-water interaction in the Sherman Granite, Wyoming and Colorado: Contributions to Mineralogy and Petrology, v. 78, p. 209-291.

NOTICE TO USERS OF INFORMATION FROM THE WYOMING STATE GEOLOGICAL SURVEY

The WSGS encourages the fair use of its material. We request that credit be expressly given to the "Wyoming State Geological Survey" when citing information from this publication. Please contact the WSGS at 307-766-2286, ext. 224, or by e-mail at wsgs.sales@wyo.gov if you have questions about citing materials, preparing acknowledgments or extensive use of this material. We appreciate your cooperation.

Individuals with disabilities who require an alternative form of this publication should contact the WSGS. For the TTY relay operator call 800-877-9975.

For more information about the WSGS or to order publications and maps, go to www.wsgs.uwyo.edu, call 307-766-2286, ext. 224, or e-mail wsgs.sales@wyo.gov

NOTICE FOR OPEN FILE REPORTS PUBLISHED BY THE WSGS

This Wyoming State Geological Survey (WSGS) open file report has not been technically reviewed or edited for conformity with WSGS standards or Federal Geographic Data Committee digital cartographic standards. Open file reports are preliminary and usually require additional fieldwork and/or compilation and analysis; they are meant to be a first release of information for public comment and review. The WSGS welcomes any comments, suggestions, and contributions from users of the information. Contact the WSGS.

DISCLAIMERS

Users of these maps are cautioned against using the data at scales different from those at which the maps were compiled. Using this data at a larger scale will not provide greater accuracy and is, in fact, a misuse of the data.

The Wyoming State Geological Survey (WSGS) and the State of Wyoming make no representation or warranty expressed or implied, regarding the use, accuracy, or completeness of the data presented herein, or of a map printed from these data. The act of distribution shall not constitute such a warranty. The WSGS does not guarantee the digital data or any map printed from the data to be free of errors or inaccuracies.

The WSGS and the State of Wyoming disclaim any responsibility or liability for interpretations made from these digital data or from any map printed from these digital data, and for any decisions based on the digital data or printed maps. The WSGS and the State of Wyoming retain and do not waive sovereign immunity.

The use of or reference to trademarks, trade names, or other product or company names in this publication is for descriptive or informational purposes only, or is pursuant to licensing agreements between the WSGS or State of Wyoming and software or hardware developers/vendors, and does not imply endorsement of those products by the WSGS or the State of Wyoming.

Best Ranch 1:24000 Quad STATEMAP Project 2010-01

By

Bagdonas, D.A., Mclaughlin J.F., and Ver Ploeg, A.J.

June 7, 2011

Prepared in cooperation with and research supported by the U.S. Geological Survey, National Cooperative Geological Mapping Program, under Cooperative Agreement G10AC00416

Introduction

The Best Ranch 1:24,000 Quadrangle contains sixteen distinct geological units ranging from Quaternary to Middle Proterozoic in age. Several units have unique characteristics, alterations, or features when compared to type sections or outcrops and require further geological description. This report includes thin section, hand sample, and outcrop pictures and analysis.

Thin sections were prepared by Spectrum Petrographics (Vancouver, Wa), interpreted by Bagdonas, D.A. and Mclaughlin J.F. Thin section were photographed by Bagdonas, D.A. and Mclaughlin J.F. using a Nikon Optiphot-P01 microscope equipped with a Nikon Coolpix 4300 digital camera.

Hand samples were collected, prepared, analyzed, and photographed by Bagdonas, D.A., Mclaughlin J.F., and Ver Ploeg, A.J. Outcrop photographs were taken by Bagdonas, D.A., Mclaughlin J.F., and Ver Ploeg, A.J.

Location:

The Best Ranch 1:24,000 Quadrangle is located on the southern edge of Albany County, Wyoming, located in the Townships 12 and 13 North, and Ranges 72 and 73 West.

Accessibility:

Access to the Best Ranch 1:24000 Quadrangle, Wyoming is possible by U.S. Highway 287 approximately 14 miles south of Laramie, Wyoming. Albany County Road 316 and Albany County Road 31 (which provides access to Albany County Road 319) all provide access to the quadrangle west of U.S. Highway 287. The intersection of U.S. Highway 287 and Albany County Road 316 is located 16.5 miles south of Laramie, Wyoming on the west side of U.S. Highway 287. The intersection of U.S. Highway 287 and Albany County Road 31 is located 17.6 miles south of Laramie, Wyoming on the west side of U.S. Highway 287. The intersection of Albany County Road 31 and Albany County Road 319 is located 3.2 miles southwest along Albany County Road 31. Much of the area covered by the Best Ranch 1:24000 Quadrangle is on private land. Permission from the land owner must be obtained before entering private lands.

Geological Data

Forelle Limestone

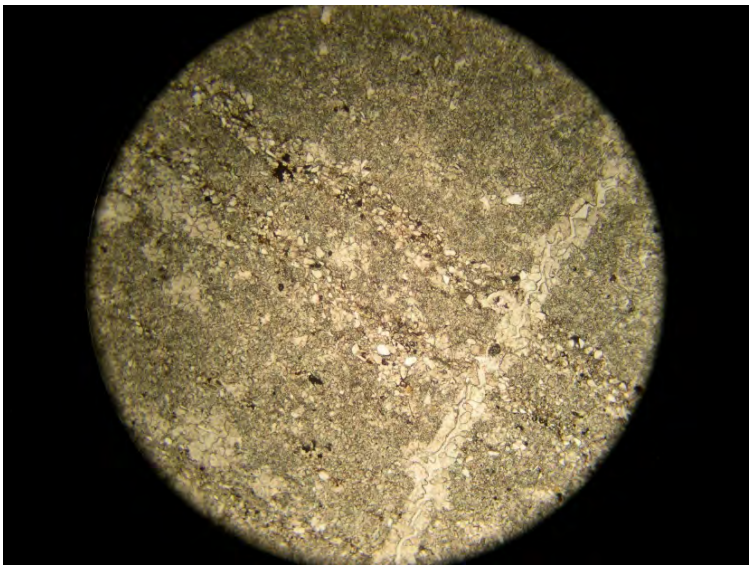

Sample 10BR4 plane-polarized light at 5X magnification:

Forelle Limestone (Permian)

Thinly bedded, limestone that is interbedded with siltstone and some gypsum veins. The limestone contains some small fossil fragments.

Thin bedding is shown as two larger grain size beds that go through the image from the top left to the bottom right.

The gypsum rich vein is the distinct lightly colored band on the right margin of the image, that cross cuts depositional bedding.

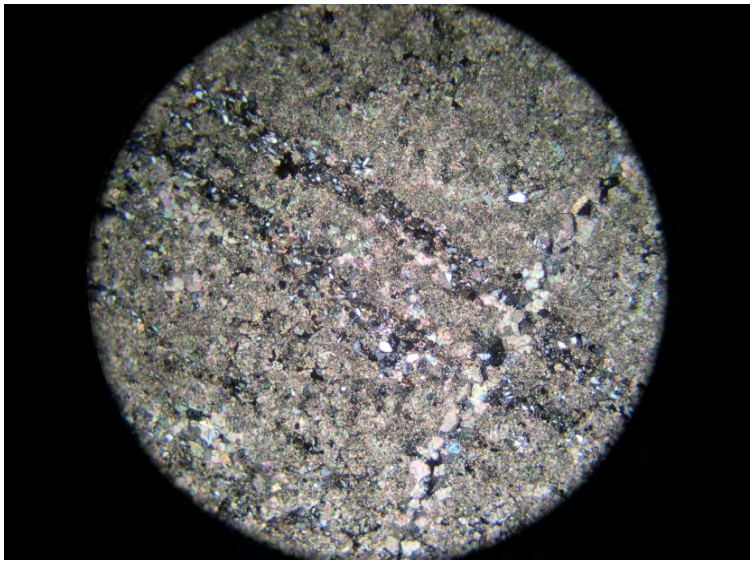

Sample 10BR4 cross-polarized light at 5X magnification:

Forelle Limestone (Permian)

Thin beds of siltstone with darker quartz rich bands. Quartz grains are subrounded to subangular. There are two bands in the image that layer the sample from top left of the image to bottom right where they are cut by a gypsum vein. The matrix surrounding the siltstone bands is primarily calcareous.

The gypsum-rich vein on the right margin of the image is highly birefringent, lacking in quartz relative to the sample and cross cuts depositional bedding.

Hand Sample 10BR4 of Forelle Limestone shows wavy algal dome structure and minor crinkly, contorted bedding that is commonly seen in the field.

Thin red siltstone layers and lenses were deposited between the calcareous layers. Siltstone layers are bedded in a similar manner to calcareous layers.

Outcrop of Forelle Limestone. The limestone outcrops as low, broken, small ridges and domes, as highly fractured beds. Note hammer for scale.

Outcrop and sample location of 10BR4 is located in T 13 N., R 73 W., Sec. 7, SSW along Albany County Road 316 (Sportman Lake Road).

Satanka Formation (Permian)

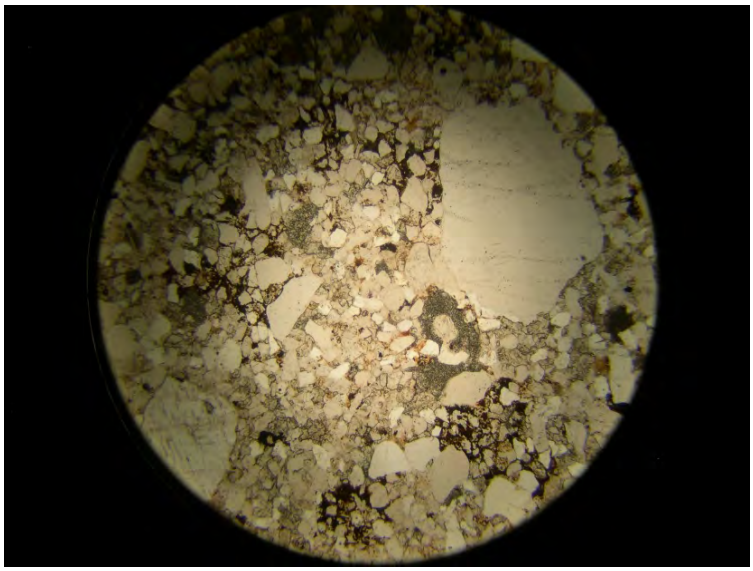

Sample 10BR19 plane-polarized light at 5X magnification:

Lower Satanka Formation (Permian)

Angular and subangular, small to medium quartz grains in a calcic cement matrix. Larger quartz and microcline grains are common in the sample.

Iron concretions are darkly cemented regions around smaller angular grains of quartz. Areas of iron concretion have less calcareous material than the rest of the sample.

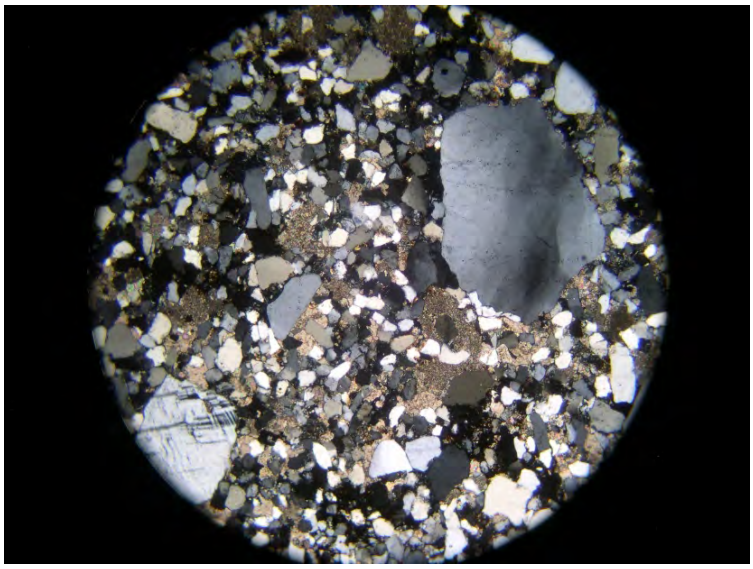

Sample 10BR19 cross-polarized light at 5X magnification:

Lower Satanka Formation (Permian)

A few larger grains of undulatory quartz and microcline are present in thin section. The undulatory quartz is a variable gray mass in the upper right of the image, while the microcline with minor scotch plaid twinning is located in the lower left of the image.

The calcic cement is very fine grained, highly birefringent, granular texture matrix around the quartz and microcline grains.

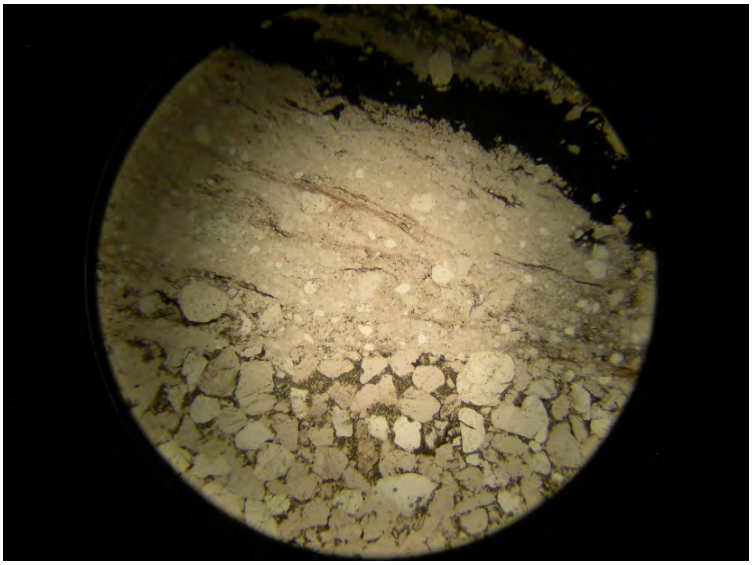

Sample 10BR18 plane-polarized light at 5X magnification:

Altered lower Satanka Formation (Permian)

Lower Satanka Formation sandstone located in close proximity to faults and fractures which experienced siliceous and iron oxide fluid alteration.

The iron-rich siliceous fluid is very fine grain, rounded, quartz grains with silica and iron cement and iron banding in the center of the veins. The portion of the sample that has had less fluid alteration still primarily contains calcic cement. The top 2/3 of the thin section is altered.

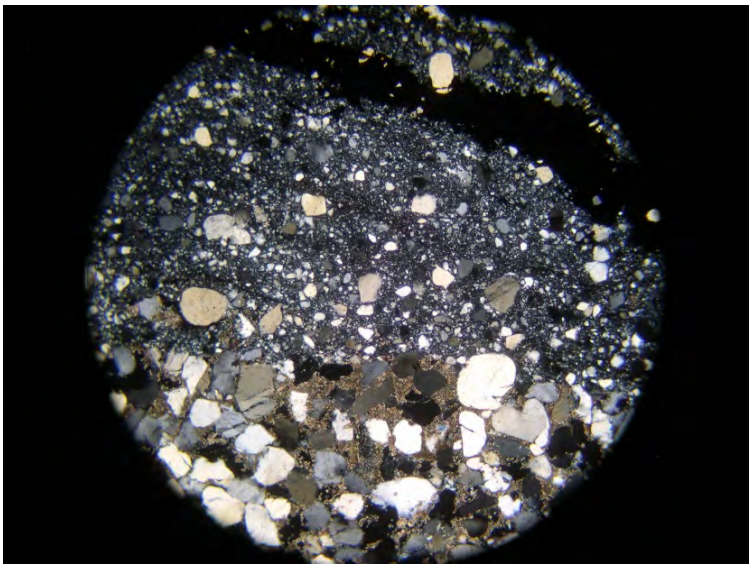

Sample 10BR18 cross-polarized light at 5X magnification:

Altered lower Satanka Formation (Permian)

In cross polarized light the, calcic cement of the less altered material is a highly birefringent ground mass around subrounded quartz grains. The lower portion of the image is less altered.

The top of the thin section lacks calcic cement and is cemented with silica and iron oxides. Fluid flow is evident as siliceous cement and iron oxide deposits oriented in a similar direction to fractures.

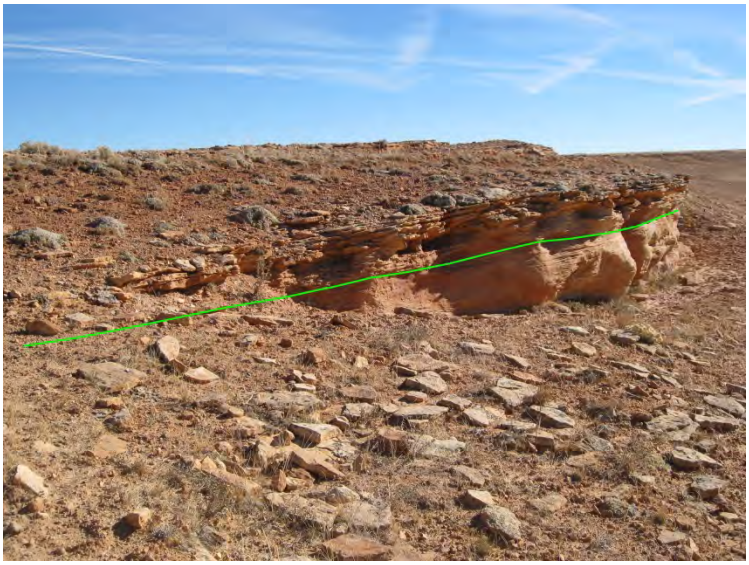

Outcrop of Satanka Formation where it contacts the Casper Formation. The Green line designates the contact between the two formations. Satanka Formation is above the line, while Casper Formation is below.

More resistant sandstone of the lower Satanka formation is underlain by Casper Formation sandstone resulting in a protruding overhang.

Casper Formation (Permian and Pennsylvanian)

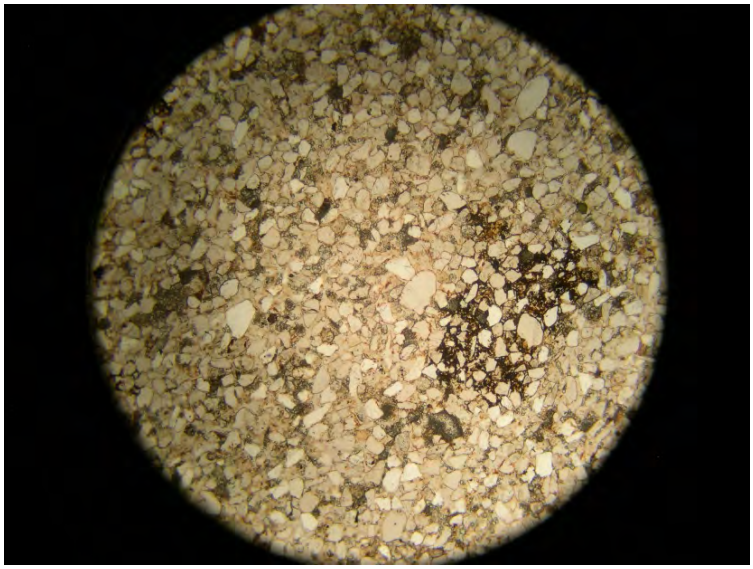

Sample 10BR3 plane-polarized light at 5X magnification:

Casper Formation (Permian and Pennsylvanian)

The Casper Formation consists primarily of fine grain, subrounded quartz grains in a calcic cement matrix. Iron concretions are seen on the margin of many quartz grains as thick opaque rims and as dark iron within the matrix of the sample.

One large iron concretion is on the right side of the thin section with several smaller iron concretions along the top and left edge.

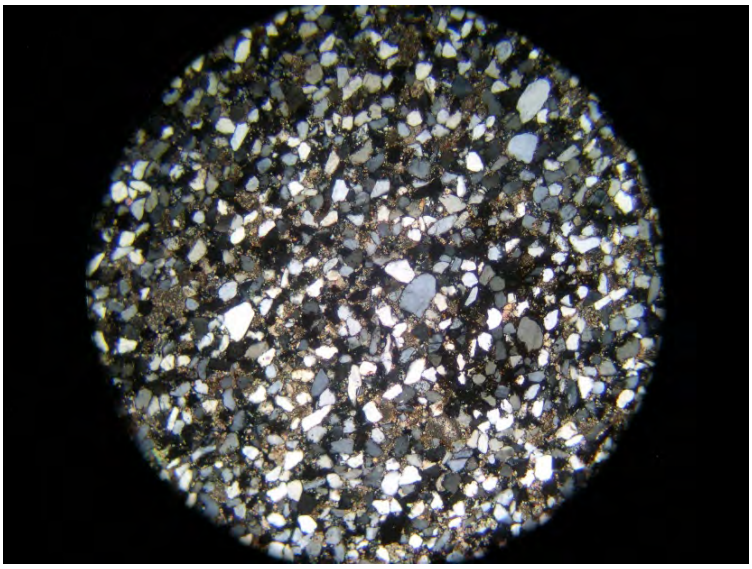

Sample 10BR3 cross-polarized light at 5X magnification:

Casper Formation (Permian and Pennsylvanian)

In cross-polarized light, the iron stained rims of the quartz grains are obvious as thick opaque margins. The calcic cement is very fine grained and lacks some birefringence due to iron staining. A few small plagioclase grains are seen in the sample as variably twinned grains.

Outcrop of Casper Formation sandstone and sample location 10BR3. The sandstone outcrops as large, meter scale festoon cross-beds. Iron concentration varies in the field from outcrop to outcrop, from red-to-pink iron-rich deposits to white and yellow iron poor deposits.

Relic fractures are filled with calcic cement with partial iron replacement in iron rich beds. Along more recent faults and fractures, the cement is siliceous and rich in iron oxides.

Sample 10BR20 plane-polarized light at 10X magnification:

Altered Casper Formation (Permian and Pennsylvanian)

This sandstone is located in close proximity to fractures and faults. Calcic cement has been replaced with silica from a silica-rich fluid alteration event. A noticeable lack of iron staining is evident in thin section. This sample location was probably lacking significant iron saturation prior to fluid alteration. This resulted in less iron oxide mobilization during alteration, as compared to other a outcrops in the map area.

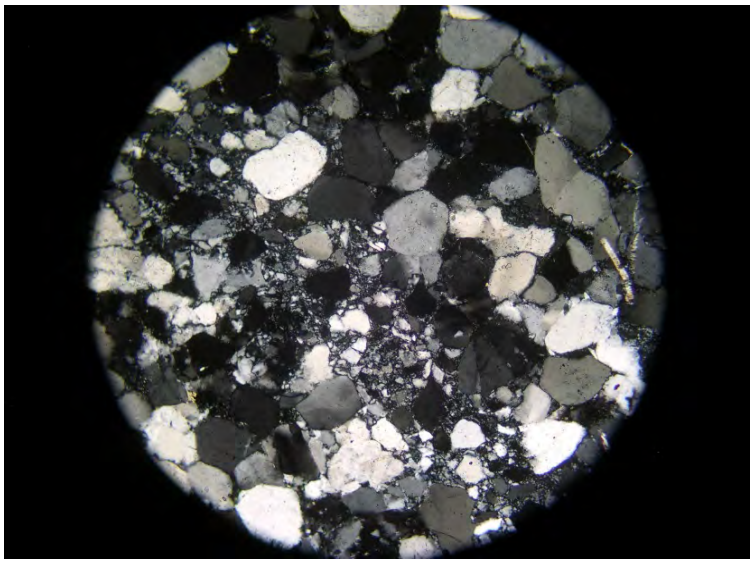

Sample 10BR20 cross-polarized light at 10X magnification:

Altered Casper Formation (Permian and Pennsylvanian)

Siliceous fluid alteration is identified as a very fine grain, rounded, quartz rich vein that cuts the image diagonally from top left to bottom right.

The larger rounded and subrounded grains of the sandstone have had the matrix of calcic cement replaced with silica cement during the fluid alteration.

Fountain Formation (Pennsylvanian)

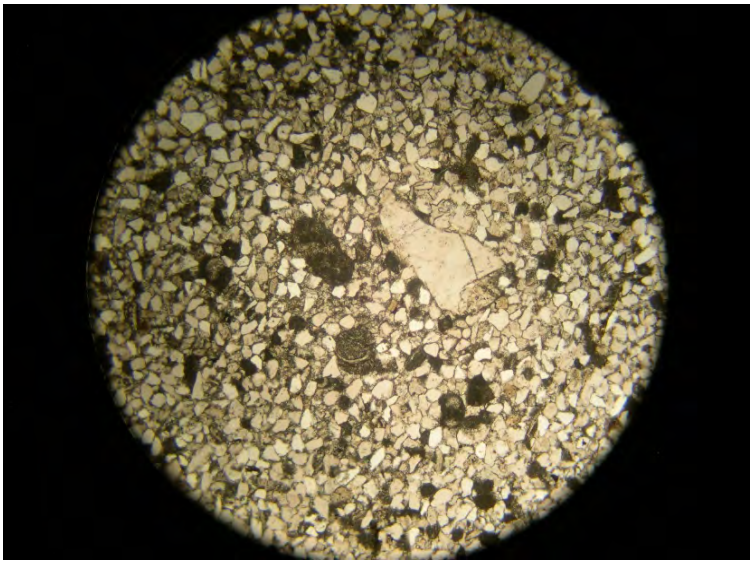

Sample 10BR1 plane-polarized light at 5X magnification:

Fountain Formation (Pennsylvanian)

Angular and subangular, fine grained, quartz and plagioclase grains that are heavily iron stained around the rims and cemented with a calcic matrix. Some larger arkosic, quartz, and limestone shell fragments are included.

Iron concretions are evident as darkly cemented areas, especially on the left margin of the image.

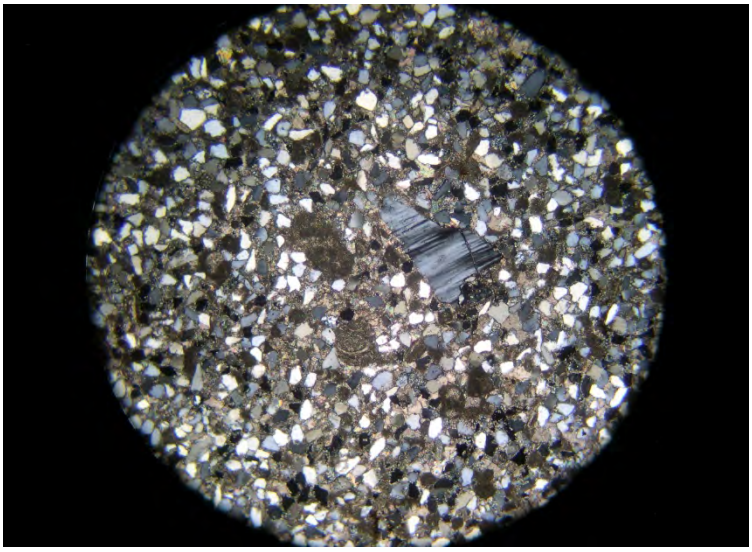

Sample 10BR1 cross-polarized light at 5X magnification:

Fountain Formation (Pennsylvanian)

In cross-polarized light, the calcic cement is evident as highly birefringent ground mass between small quartz and arkosic grains. The calcic cement inner grows many crystal margins.

A large plagioclase grain is seen with basic twinning in the center of the image. Margins of the plagioclase grain exhibit calcic cement that is beginning to invade the structure of the grain.

Hand Samples 10BR1 of Fountain Formation

Hand samples of 10BR1, an arkosic, fine to medium grained sandstone that exhibits mottled iron spotting and layering, as well as lenses of shell fragments and larger-grained sands.

Outcrop of Fountain Formation where sample 10BR1 was collected. It is arkosic sandstone with mottled iron staining and lenses of larger grain sands and shell fragments.

Outcrop of Fountain Formation and sample locations for both 10BR1 and 10BR2.

Sample 10BR1 was taken from the ledge-forming meter thick band of arkosic sandstone. Up section from the arkosic sandstone is a thinly bedded limey sandstone. It is seen as a thin, ledge forming band above the dominant ledge, and is the source locality for sample 10BR2.

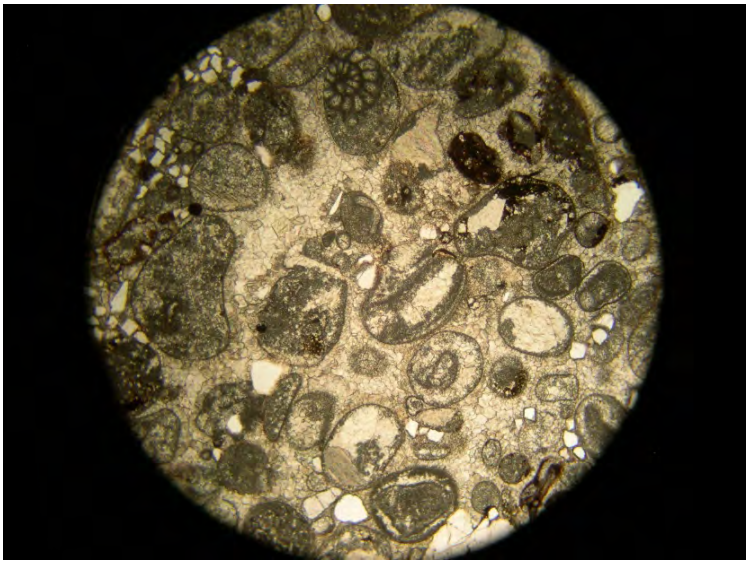

Sample 10BR2 plane-polarized light at 10X magnification:

Fountain Formation (Pennsylvanian)

Medium grained, rounded to well-rounded calcic fragments including shells and oolitites. Some smaller subrounded to subangular quartz grains are seen in thin section.

Calcic cement makes up the matrix of the sample.

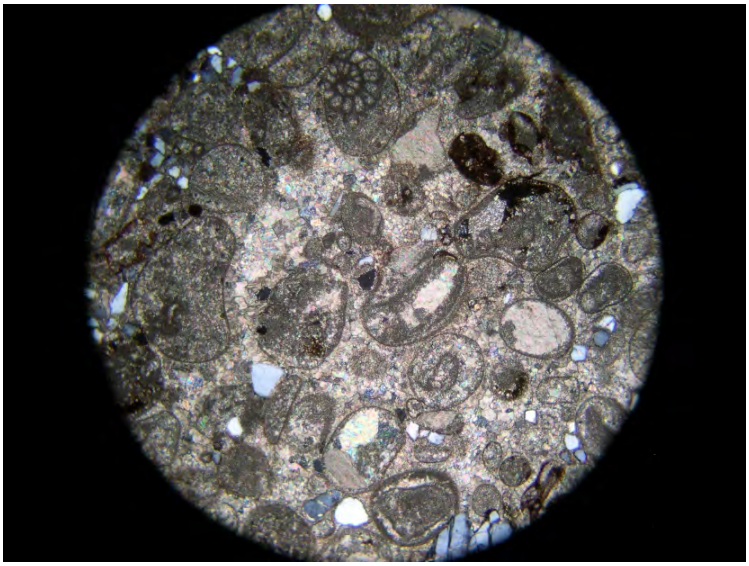

Sample 10BR2 cross-polarized light at 10X magnification:

Fountain Formation (Pennsylvanian)

As seen in cross polarized light, the sample is predominately calcic. Only a few quartz grains and iron stains are seen.

Quartz grains are located along the margins of the image as white-to-gray subangular grains.

Outcrop of Fountain Formation where sample 10BR2 was collected.

The outcrop contains limey shell fragments in thin laminar bedding throughout this member of the Fountain Formation. There is very little siliceous material in this sample.

Monzodiorite dike (Mg-rich)

10BR17 plane-polarized light at 5X magnification:

Magnesium-rich monzodiorite dike

Magnesium rich monzodiorite dikes contain tabular xenocrysts of compositionaly zoned plagioclase and perthite. Abundant, very small, needle-shaped apatite are pervasive throughout the sample and are seen in thin section.

Major Phases include plagioclase (some as myrmekite), perthite, microcline, biotite (sometimes altered to chlorite), hornblende, quartz, and orthoclase.

Minor Phases include apatite, epidote, ilmenite, magnetite, titanite, and zircon.

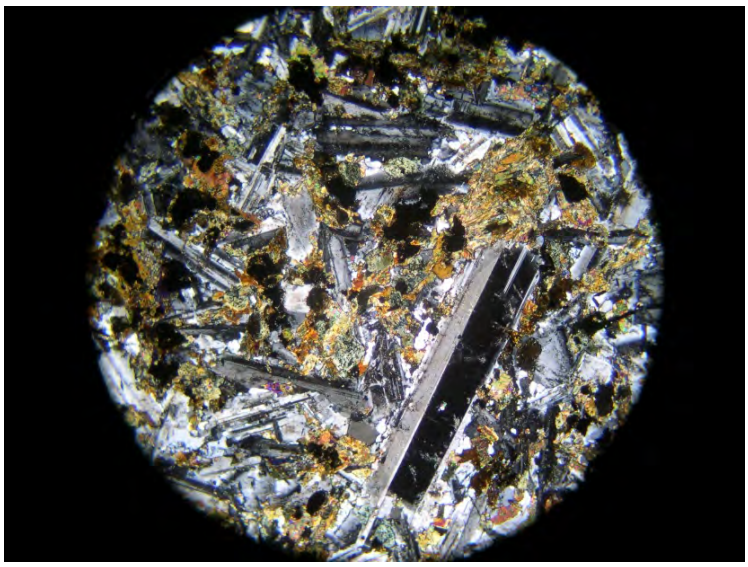

10BR17 cross-polarized light at 5x magnification:

Magnesium-rich monzodiorite dike

In cross polarized light the large tabular xenocryst of plagioclase is seen in the right portion of the image.

Alteration of the sample is evident as abundant epidote, iron-oxide staining, chlorite, and in some cases, minor secondary quartz that was carried by a silica rich fluid.

Outcrop of magnesium-rich monzodiorite dike and sample location for 10BR11.

The sub-vertical orientation of jointing in the outcrop is representative of the near vertical emplacement orientation of the magnesium rich dikes in the map area. This orientation is also similar to magnesium rich monzodiorite dikes throughout the Sherman batholith.

Lincoln Granite

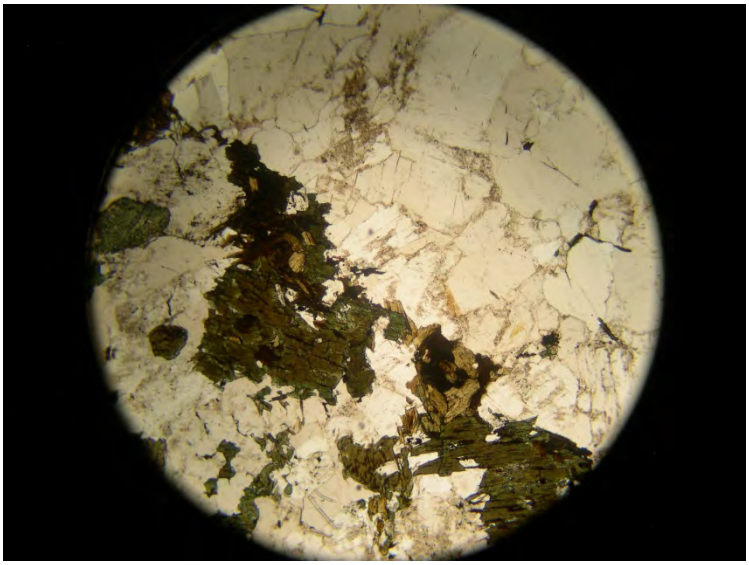

Sample 10BR11 plane-polarized light at 5X magnification:

Lincoln Granite

Major Phases include quartz, plagioclase, microcline, perthite, biotite, hornblende, and ilmenite.

Minor Phases include apatite, zircon, myrmekite.

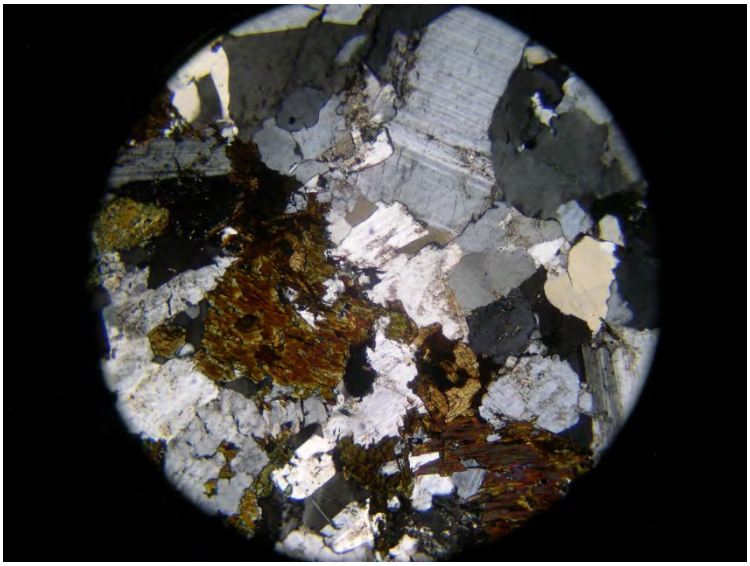

Sample 10BR11 cross-polarized light at 5X magnification:

Lincoln Granite

Quartz and plagioclase are abundant in the upper right portion of the image.

The bottom left portion of the image contains larger hornblende grains with smaller biotite and ilmenite grains inner grown on the hornblende margins.

Outcrop of Lincoln granite contacting the Sherman granite. The Lincoln granite makes up the top half of the outcrop and is seen as a distinctly finer-grained, blocky granite.

Contacts of Lincoln granite with Sherman granite are generally sharp.

Monzodiorite dikes and pods (Fe-rich)

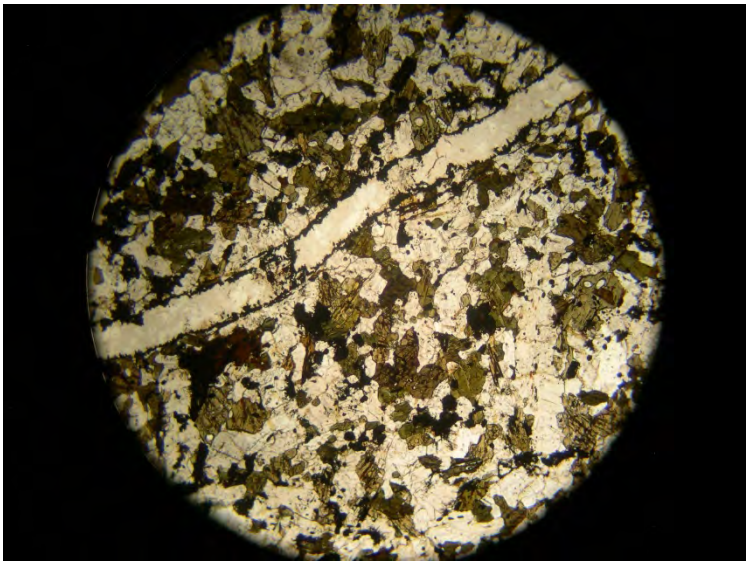

Sample 10BR13 plane-polarized light at 5X magnification:

Iron-rich monzodiorite

Iron rich dikes and pods are commingled with Porphyritic granite and Lincoln granite and are generally emplaced as enclave-like dike features.

Major Phases include plagioclase, perthite, biotite, quartz, and orthoclase.

Minor Phases include titanite, apatite, ilmenite, magnetite and zircon.

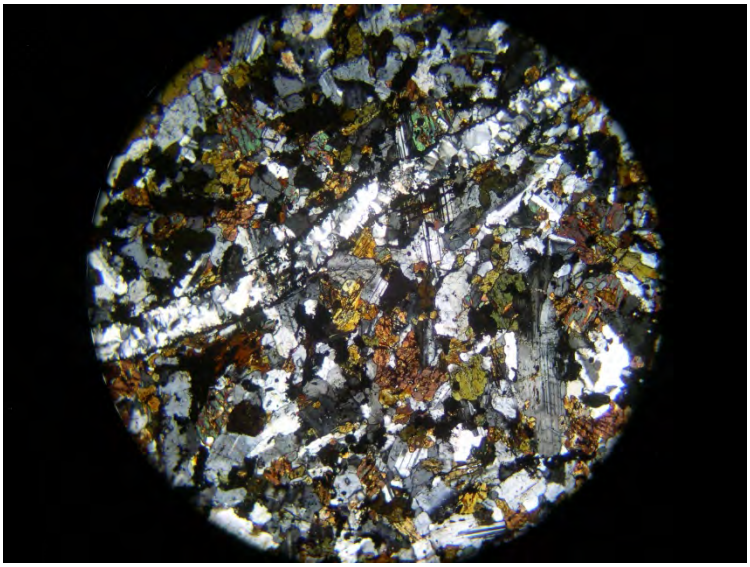

Sample 10BR13 cross-polarized light at 5X magnification:

Iron-rich monzodiorite

The iron rich monzodiorite dike has been cross cut by a leucocratic vein during late stage batholith cooling.

The leucocratic vein is primarily quartz and iron oxides. Margins of the vein are primarily iron oxides that have leached from the country rock into the vein during later alteration.

Outcrop of iron-rich monzodiorite dike where leucocratic material similar to the Lincoln granite has intruded the dike.

Porphyritic Granite

Sample location 10BR8.

Porphyritic granite

Major Phases of the Porphyritic granite include perthitic microcline, plagioclase, orthoclase, quartz, biotite, and hornblende.

Minor Phases include ilmenite, apatite, zircon, titanite, and pigeonite.

Outcrop of Porphyritic granite, Sample location 10BR14 that has undergone moderate hydrothermal alteration.

Much of the Porphyritic granite in the map area has undergone some degree of hydrothermal alteration. Alteration increases as outcrops become more proximal to major faults.

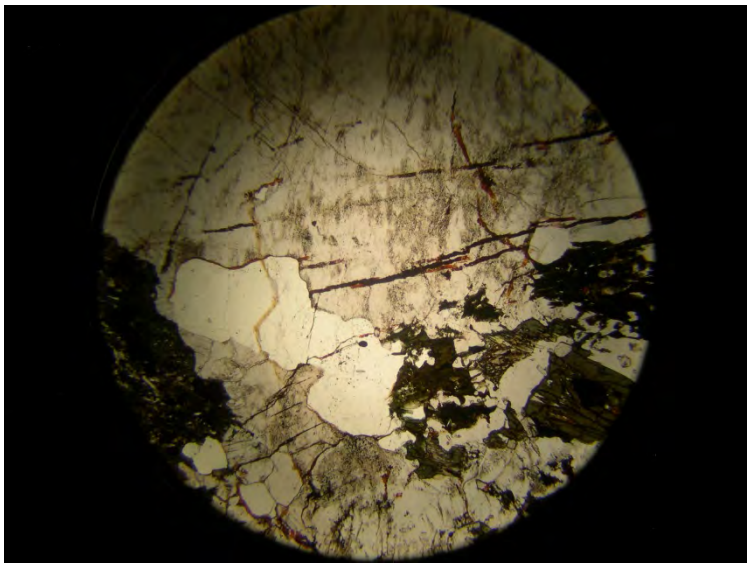

Sample 10BR8 plane-polarized light at 5X magnification:

Porphyritic granite

Major Phases of the Porphyritic granite include perthitic microcline, plagioclase, quartz, biotite, and hornblende.

Minor Phases include ilmenite, apatite, zircon, and titanite.

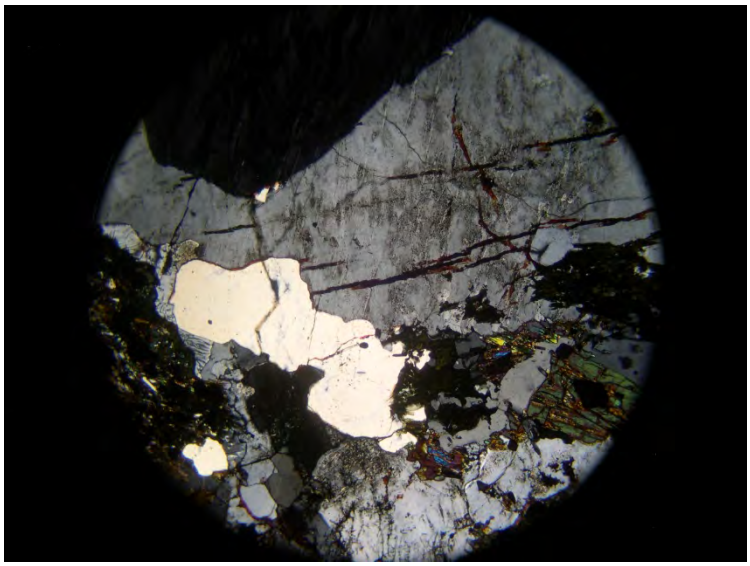

Sample 10BR cross-polarized light at 5X magnification:

Porphyritic granite

Hydrothermally altered rapakivi texture where perthitic cores have been altered to a very fine grain, feathery mass of sericite. Epidote and minor chlorite are also identified as alteration products. Biotite exhibits moderate chloritic alteration with fine grain, secondary quartz growth that de-laminates cleavage plains. Hematite rich fluid is evident on crystal margins.

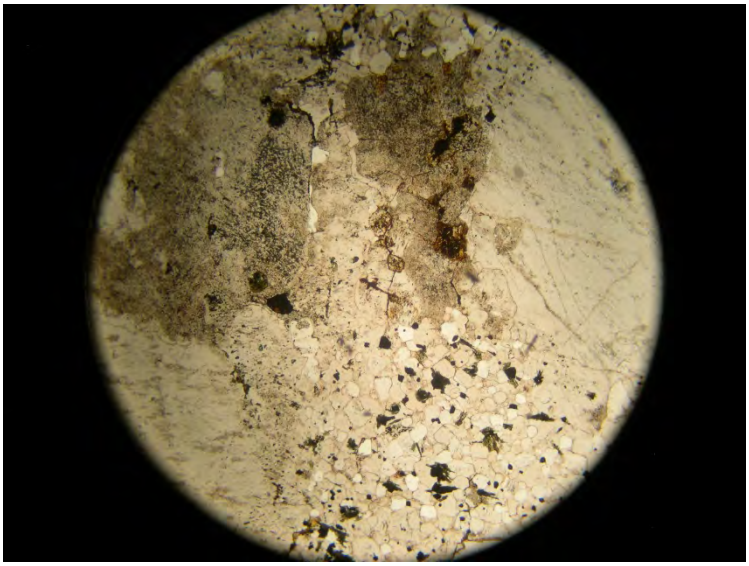

Sample 10BR14 plane-polarized light at 5X magnification:

Severely altered Porphyritic granite

Major Phases of the Porphyritic granite are perthitic microcline, plagioclase, quartz, biotite, hornblende, *and in hydrothermally altered samples, epidote, and chlorite.*

Minor Phases include ilmenite, apatite, zircon, titanite, *and in hydrothermally altered samples sericite, hematit, and hydrothermally associated secondary quartz.*

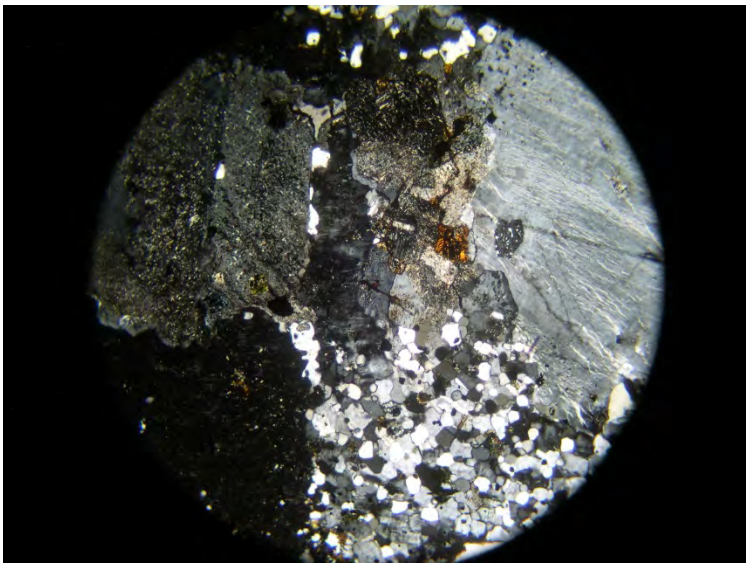

Sample 10BR14 cross-polarized light at 5X magnification:

Severely altered Porphyritic granite

Perthitic cores have large amounts of feathery sericite while rapikivi rims have been altered to epidote, chlorite, and secondary quartz. Small plagioclase and quartz inclusions are abundant in perthitic porphryoclasts. Iron staining is noticeable as dark colored areas both in and around plagioclase and perthite grains.

Sherman Granite

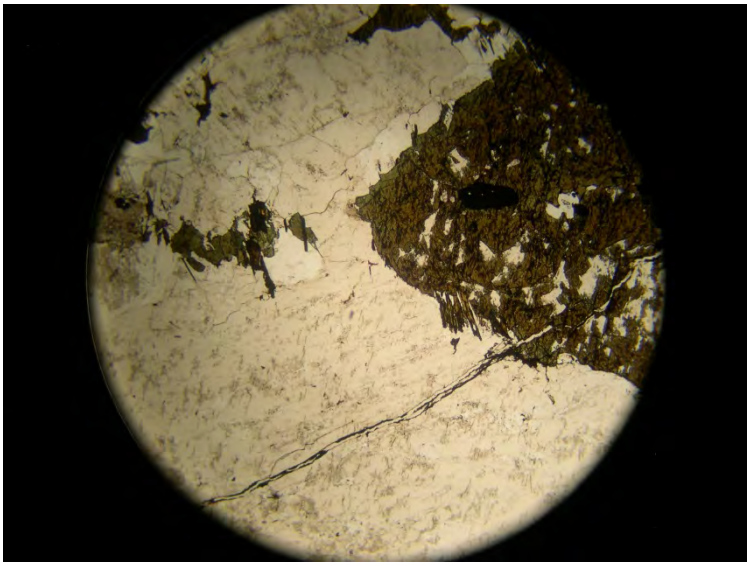

Sample 10BR7 plane-polarized light at 5X magnification:

Sherman granite

Major Phases include microcline, plagioclase, perthite, quartz, hornblende, biotite, and ilmenite.

Minor Phases include zircon and apatite, and in some locations fayalite.

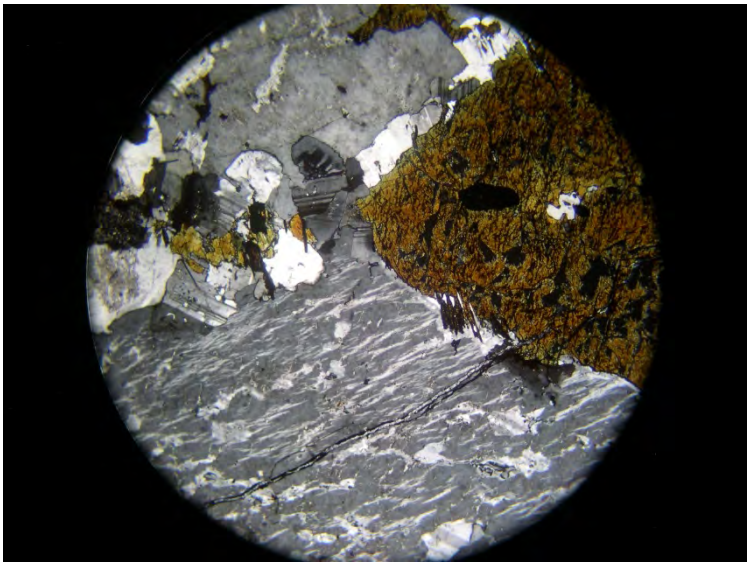

Sample 10BR7 XP 5X

Sherman granite

The Sherman granite has a subporphyritic granular texture, exhibiting megacrystic microcline and perthite rimmed in plagioclase, some orthoclase, and quartz. Rapakivi-texture is common in Sherman granite.

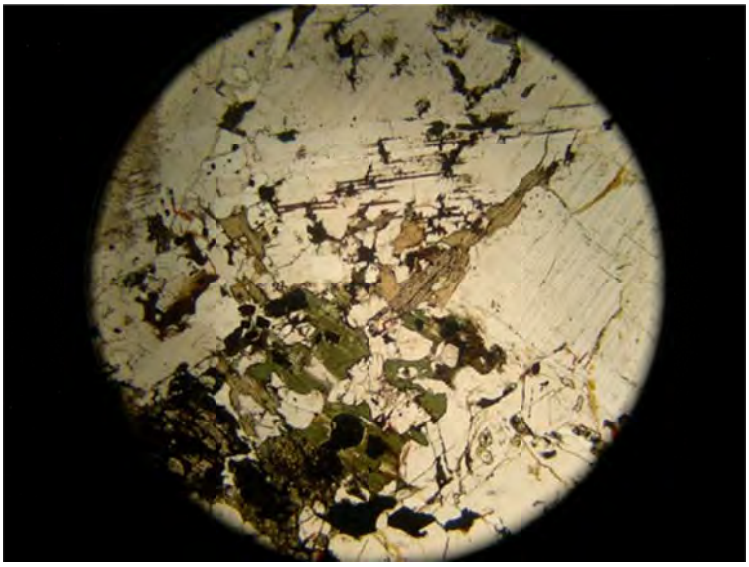

Sample 10BR9 plane-polarized light at 5X magnification:

Hybridized and moderately altered Sherman granite is located along Willow Creek in the eastern portion of the map area. It is associated with a large hydrothermal alteration zone and has been hybridized with iron-rich mafic enclaves and pods.

Major Phases include microcline, perthite, plagioclase, hornblende, quartz, biotite, ilmenite, and apatite.

Minor Phases include epidote as an alteration product, zircon, and titanite.

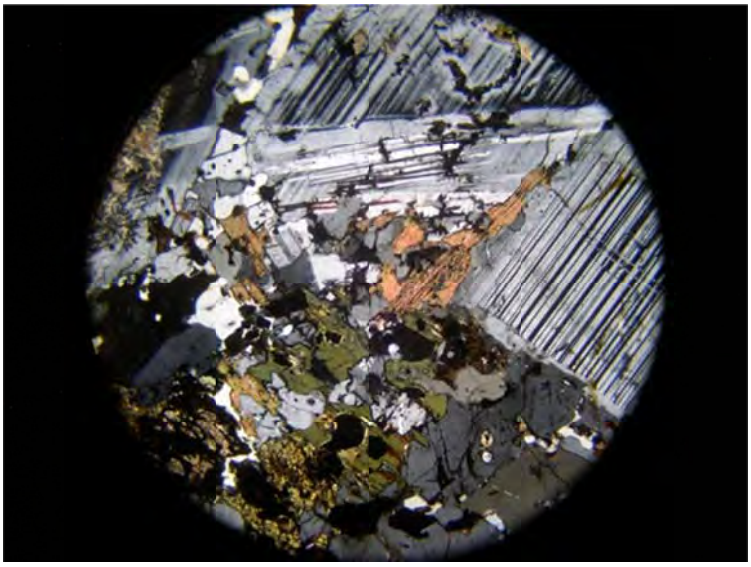

Sample 10BR9 cross-polarized light at 5X magnification:

Large grain phenocrysts of anti-rapakivi plagioclase are surrounded by a finer grain matrix of perthite, plagioclase, orthoclase and quartz. Inner grown quartz, biotite, and hornblende surround the porphyry mass.

Outcrop of hybridized and moderately altered Sherman granite with rapikivi-texture and emplacement oriented phenocrysts. Sample location for 10BR9**.**

Additional Geological Data

Uplifted Fountain Formation limestone bed. Outcrop of Fountain formation that was tilted or folded by reverse faulting.